Excitatory synaptic inputs to spiny stellate cells in cat visual cortex

K. J. Stratford, K. Tarczy-Hornoch, K. A. C. Martin*, N. J. Bannister & J. J. B. Jack

University Laboratory of Physiology, Parks Road, Oxford OX1 3PT, UK
* Institute of Neuroinformatics, ETH and University of Zurich, Gloriastrasse 32, 8006 Zurich, Switzerland

In layer 4 of cat visual cortex, the monocular, concentric receptive fields of thalamic neurons, which relay retinal input to the cortex, are transformed into 'simple' cortical receptive fields that are binocular and selective for the precise orientation, direction of motion, and size of the visual stimulus[1]. These properties are thought to arise from the pattern of connections from thalamic neurons[1–6], although anatomical studies show that most excitatory inputs to layer 4 simple cells are from recurrently connected circuits of cortical neurons[7–9]. We examined single fibre inputs to spiny stellate neurons in slices of cat visual cortex, and conclude that thalamocortical synapses are powerful and the responses they evoke are unusually invariant for central synapses. However, the responses to intracortical inputs, although less invariant, are strong enough to provide most of the excitation to simple cells *in vivo*. Our results suggest that the recurrent excitatory circuits of cortex may amplify the initial feedforward thalamic signal, subserving dynamic modifications of the functional properties of cortical neurons[10–12].

In cat visual cortex, spiny stellate neurons are the primary target of the lateral geniculate nucleus (LGN) neurons that relay retinal signals to the primary visual cortex[7,8,13–16]. Their dendrites, which are confined to layer 4, receive synaptic input only from axons forming boutons in layer 4 (refs 9,14,17). Excitation comes mainly from LGN relay neurons, layer 6 pyramidal neurons, and other layer 4 spiny neurons[9,14–18]. Within layer 4, the axons of layer 6 pyramidal neurons and layer 4 spiny neurons provide about 8 and 5 times as many synaptic contacts, respectively, as LGN neurons[9]. To investigate the properties of these different excitatory synapses, we recorded intracellularly *in vitro* from layer 4a spiny stellate neurons, and evoked fast excitatory postsynaptic potentials (EPSPs) by minimal extracellular stimulation[19,20] of single afferent axonal fibres. By varying the position of the stimulating electrode we explored the multiple, convergent intracortical and subcortical inputs to a given cell. By using paired recording, we then investigated the excitatory connections between pairs of layer 4 neurons, and between layer 6 and layer 4 neurons.

The minimal-stimulation data are from 21 neurons with spiny stellate morphology (Fig. 1), recorded with γ-aminobutyric acid ($GABA_A$) receptor-mediated inhibition and NMDA (*N*-methyl-D-asparate) receptor-mediated excitation blocked, and with 2.5 mM Ca^{2+} and 1 mM Mg^{2+}. Multivariate cluster analysis[21] of 48 inputs showed that they clustered optimally into three classes (Table 1). Class 1 EPSPs (Fig. 1) had large mean amplitudes with low coefficients of variation (CVs), and short response latencies. Stimulation often resulted in failure, alternating on successive trials between the first and second paired pulse; stronger stimulation or longer intervals reduced second-pulse failures, suggesting that these axons are relatively refractory to extracellular stimulation. Paired pulses following successful first pulses were usually depressed in amplitude. In contrast, Class 3 EPSPs (Fig. 2), with high CVs, small mean amplitudes, and longer response latencies, showed paired-pulse facilitation (8 of 12), with a time course consistent with that reported for other cortical neurons[22], peaking around 15 ms. Class 2 EPSPs (Fig. 3*a–d*) showed intermediate CVs and amplitudes, latencies similar to those of class 3 EPSPs, and slight depression or no change for paired pulses.

There were several indications that the three classes of synaptic response might be correlated with the three major anatomical sources of excitation to spiny stellate neurons[9]. Class 1 inputs had the shortest response latencies, despite distant sites of stimulation,

TABLE 1 Summary of statistics for EPSPs of different synaptic classes

	Class 1	Class 2		Class 3	
		Minimal stimulation	Dual recording	Minimal stimulation	Dual recording
Number	20	18	14	10	7
Amplitude (μV)	1,970 ± 1,447 (387–5,887)	1,042 ± 568 (307–2,022)	1,072 ± 689 (178–2,205)	334 ± 217 (123–788)	226 ± 153 (80–473)
CV (%)	8.3 ± 3.9 (−2.5–16.5)	12.2 ± 7.6 (0–31.4)	21.6 ± 10.1 (9.4–39.9)	47.0 ± 13.9 (5.5–72.0)	68.6 ± 28.4 (24.1–109.9)
Rise time (ms)	1.1 ± 0.5 (0.4–1.8)	1.4 ± 0.3 (0.8–1.8)	1.1 ± 0.4 (0.8–1.8)	1.4 ± 0.5 (0.8–2.0)	1.4 ± 0.3 (1.0–1.6)
Half width (ms)	8.8 ± 4.7 (3.2–13.2)	8.4 ± 2.7 (4.8–12.2)	10.7 ± 4.2 (5.4–17.8)	7.8 ± 2.0 (4.8–10.2)	12.7 ± 5.7 (8.4–21.0)
Latency (ms)	1.1 ± 0.3 (0.6–1.8)	1.7 ± 0.7 (0.8–3.0)		1.7 ± 0.7 (1.0–3.4)	
AQD	0.17 ± 0.08 (0.06–0.30)	0.44 ± 0.04 (0.34–0.56)	0.36 ± 0.07 (0.23–0.45)	0.41 ± 0.04 (0.32–0.47)	0.41 ± 0.03 (0.37–0.46)

For each synaptic input the following variables were recorded: amplitude (mean amplitude of successful responses to first stimulus at 1 Hz averaged for all available stimulus trials); CV (defined as $(\sigma_s^2 - \sigma_n^2)^{1/2}/\mu_s$, excluding stimulation failures, and expressed as a percentage (in two cases the EPSP variance was less than that of the noise, and CVs were defined as $-(\sigma_s^2 - \sigma_n^2)^{1/2}/\mu_s$); rise time (time for rising phase of EPSP from 10% to 90% of peak amplitude); half width (time between 50% peak amplitude on rising phase and 50% on falling phase of EPSP); latency (time from onset of stimulus activation to onset of EPSP); and average quadrant deviation (AQD) (see Fig. 1 legend). All figures are shown as mean ± standard deviation (minimum – maximum). The 48 synaptic inputs from minimal-stimulation experiments were analysed with a program that performed cluster analysis[21]. Using the parameters of coefficient of variation, latency, direction of paired-pulse change (depression or facilitation defined as greater than 10% change), and AQD in assessing the clustering criterion, it was found that allowing three classes gave the optimal categorization of the inputs, as apparent from a marked inflection in the plot of the clustering criterion as a function of the number of groups[21]. The sample numbers do not reflect the true prevalence of each class of input, because we selected positively for the large-amplitude class 1 and class 2 inputs, although class 3 inputs were actually most common. Class 2 and class 3 extracellularly evoked EPSPs are very similar to EPSPs recorded in dual impalements from layer 4 and layer 6 presynaptic neurons, respectively. The tendency of extracellularly evoked inputs in each group to have lower CVs than the corresponding dual-recording group is caused by the requirements of a rigorous minimal-stimulation protocol, which generally biases acceptance in favour of less variable inputs. In dual recordings it was not possible to measure latency, as the EPSP onset was obscured by the presynaptic spike artefact. This may also have affected the rise-time measurement.

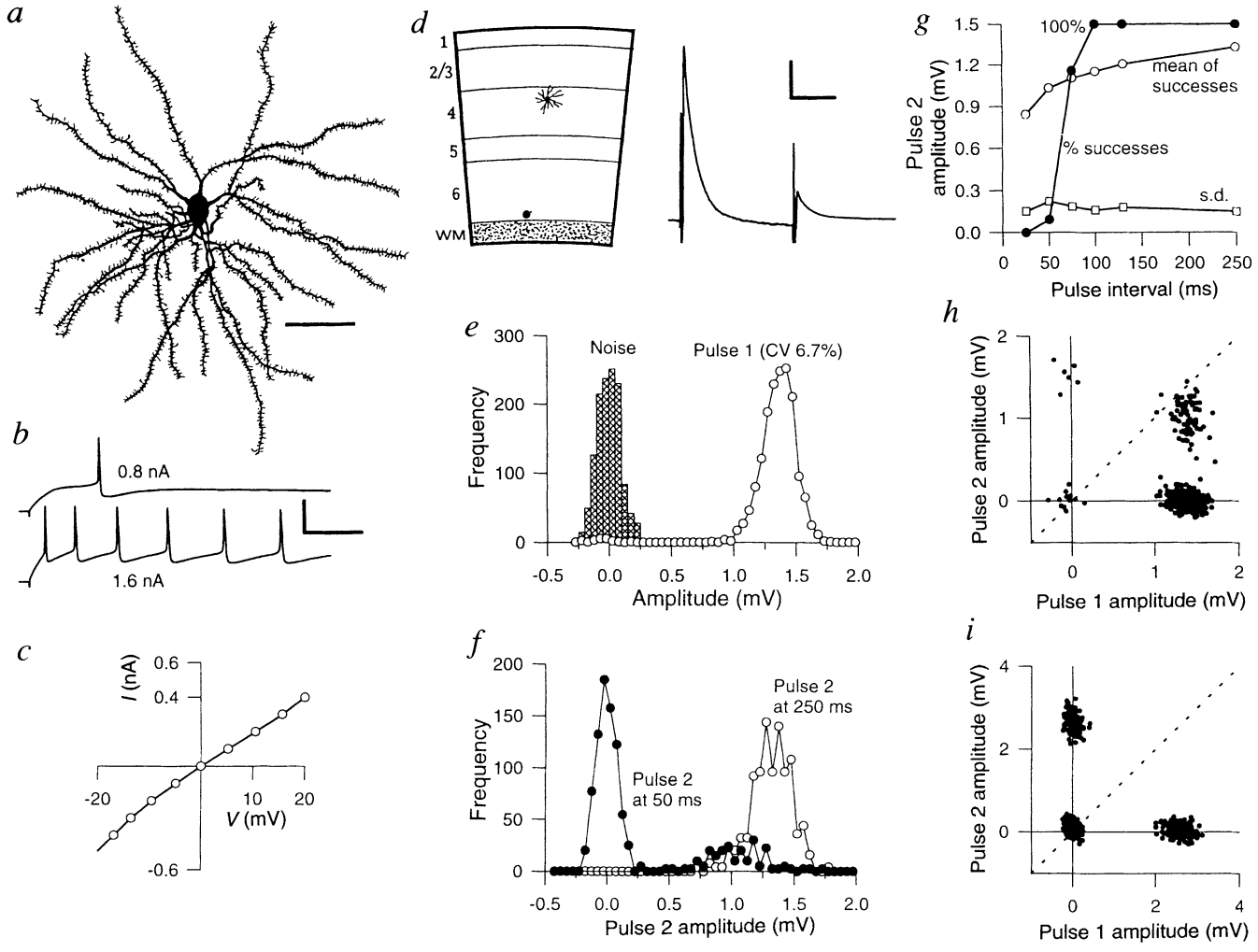

FIG. 1 Class 1 inputs. *a*, Camera lucida reconstruction of a spiny stellate neuron from which the data in *b–h* were recorded. Scale bar, 50 μm. *b*, Firing responses to 0.8 nA and 1.6 nA current pulses. Scale bar, 30 ms, 50 mV. *c*, Current–voltage relation (100-ms current steps; origin −76 mV). Average resting potential, input resistance and membrane time constant of cells (2 M electrodes) were −56 mV, 63 MΩ, and 16 ms (holding potential −80 mV). *d*, Left, positions of layer 4 neuron, and stimulating electrode at border of layer 6 and white matter (WM) (50 μm off-radial towards the LGN) for the input described in *d–h* (1,650 trials recorded). Right, averaged EPSP is of large amplitude; averaged response to second pulse is small owing to stimulation failures. With membrane depolarization (data not shown), amplitudes became smaller (CVs invariant), consistent with passive membrane properties, suggesting that large amplitudes were not from activation of voltage-dependent dendritic Na^+ or Ca^{2+} channels. Scale bar, 20 ms, 300 μV. *e*, Amplitude histograms of noise and pulse-1 response: $\sigma_n = 82\,\mu V$, $\mu_{s1} = 1{,}373\,\mu V$, and $\sigma_{s1} = 123\,\mu V$; noise-corrected CV 6.7%. *f*. Pulse-2 response at 50 ms (filled circles) and 250 ms (open circles) paired-pulse intervals; at 50 ms, pulse 2 fails more, and responses to successful stimulation are depressed. *g*, As interpulse interval is shortened, mean amplitude of successful pulse 2 responses decreases gradually and the proportion of failures increases sharply. *h*, Scattergram of pulse-2 response (50 ms delay) against pulse-1 response; depression illustrated by points just below diagonal. *i*, Similar plot for a different class-1 input; all trials show failure on pulse 1 and/or pulse 2. To quantify these scattergram patterns, axes were divided at the mid-range of pulse-1 responses, and the mean distance of points from the centroid of the points in each quadrant, averaged over four quadrants, was normalized by quadrant size to give an average quadrant deviation score for use in cluster analysis (Table 1).

METHODS. Blocks of visual cortex (area 17) from cats 12–14 weeks old (1.0–1.3 kg) were excised by craniotomy after pentobarbitone-induced anaesthesia (Sagatal, Sigma, 60 mg per kg, intraperitoneal) maintained with intravenous Saffan. Coronal slices (400 μm thick) were maintained in an interface chamber[25], with 50 μM D L-2-amino-5-phosphopentanoic acid (AP5, Sigma) and, for minimal stimulation, 100 μM picrotoxin (Sigma). Voltage recordings of synaptic potentials and responses to current pulses in layer 4a neurons used biocytin-filled sharp intracellular microelectrodes[25] (0.5 M CH_3SO_4K filling solution for dual impalements, 2 M for minimal-stimulation experiments). A minimal-stimulation protocol[19,20] activated single afferent axons with a bipolar wire electrode (20–200 μs voltage pulses): the average evoked response as a function of stimulus intensity shows plateaux separated by step increases as individual fibres are recruited[20]; stimulus intensity was adjusted to the first plateau, provided this response showed no 'contamination' by more than one fibre (very variable latency or rise time). Responses were evoked at 1 Hz, using paired pulses (interval 50 ms or varied systematically where appropriate). In dual recording the presynaptic cell was driven to fire multiple spikes to explore paired-pulse behaviour. Synaptic responses were digitized at 5 kHz, and amplitudes of individual events were measured as differences between averages over short windows at baseline and signal peak[25]. Fixed slices were resectioned and biocytin visualized for morphological identification and reconstruction.

usually at the border between layer 6 and white matter (16 of 20). They must have arisen from rapidly conducting axons, such as the myelinated thalamic axons. These fibres are thickest, and thus easiest to activate where they enter the grey matter[18], which would explain why class 1 inputs were preferentially evoked there. Severed axons might be prone to prolonged refractoriness and hence to stimulation failures, which were observed only in class 1 inputs. Class 2 inputs could be evoked throughout layers 2–6, but were the only ones activated from layers 2 and 3. Thalamic and layer 6 pyramidal axons rarely project to superficial layers[7,13], whereas the axons of layer 4 spiny neurons project heavily into layers 2 and 3 (refs 14–16), and would be easily activated there. Layer 6 pyramidal neurons, unlike thalamic afferents, produce an augmenting response in layer 4 *in vivo*[23], possibly by means of EPSPs showing paired-pulse faciitation, like the class 3 inputs. Indeed, most (9 of 10) class 3 EPSPs were evoked radially in layers 5 and 6, where layer 6 pyramidal axons ascend. All three input classes converged on individual spiny stellate neurons, as predicted by anatomical observations[9].

We investigated this suggested structure–function correlation directly by examining the intracortical subset of inputs to layer 4 using dual intracellular recording[25]. We recorded 7 connections from layer 6 pyramids to layer 4 excitatory neurons. These EPSPs had small amplitudes and large CVs, and showed paired-pulse facilitation (7 of 7), thus closely resembling class 3 minimal stimulation inputs (Table 1 and Fig. 2*e–i*). Paired recording between excitatory cells in layer 4 yielded 14 connections onto confirmed spiny stellate neurons. Like class 2 EPSPs, these had larger amplitudes and lower CVs than the layer 6 to 4 connections, and showed depression or no change on paired pulses (Table 1 and Fig. 3*e–h*). The match between minimal stimulation and dual recording data validates the minimal-stimulation technique, and importantly allows us to attribute the physiological characteristics of class 2 and class 3 EPSPs directly to defined intracortical excitatory pathways. Class 1 EPSPs were not seen in any dual-impalement connections ($n = 51$), thus further supporting their suggested extracortical, thalamic origin: *in vitro* axons can be activated by extracellular stimulation, but are unlikely to be impaled.

The putative thalamic EPSPs show a striking combination of large amplitude and low CV, and, along with class 2 EPSPs, contradict the suggestion that cortical connections always evoke small, highly variable responses[26]. Class 1 CVs imply minimal trial-to-trial variation in the number of neurotransmitter quanta released, as if there were only one release site. However, the EPSPs are large for monoquantal responses. From EPSP time

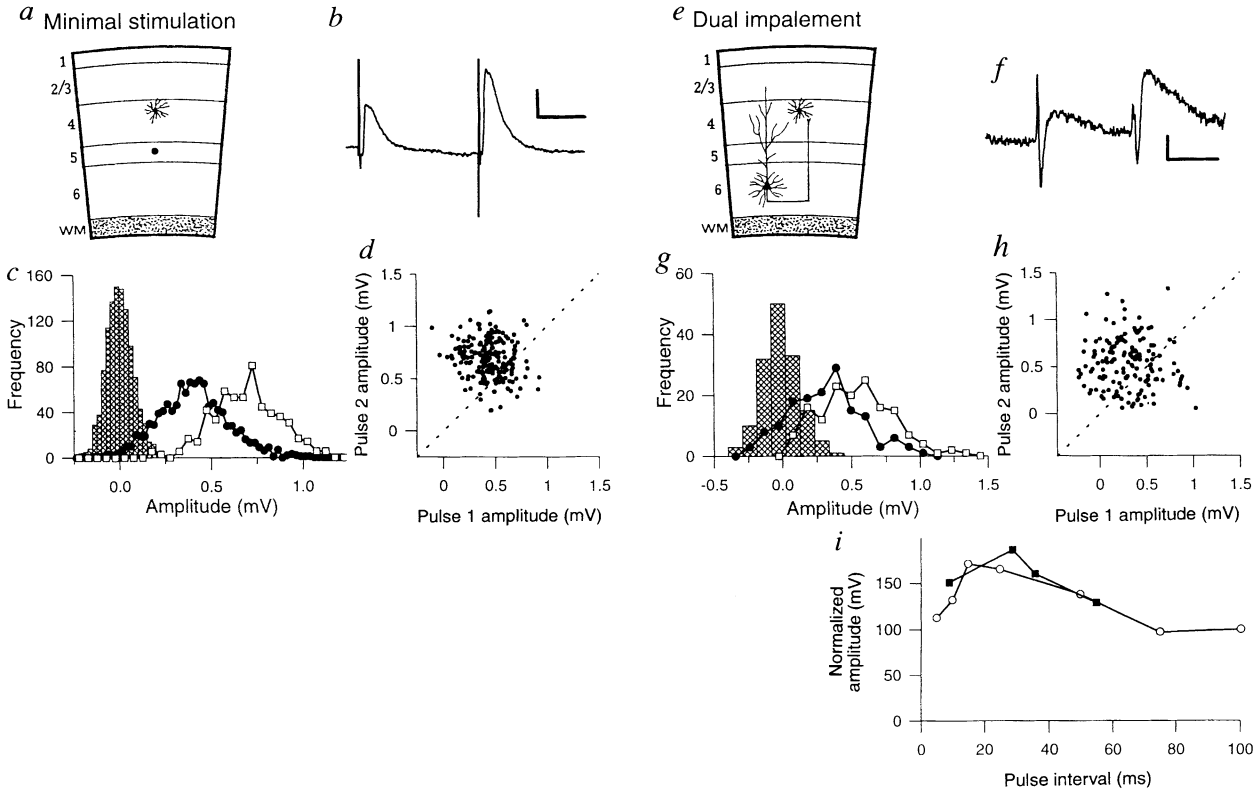

FIG. 2 Class 3 inputs. Characteristics of class 3 synaptic inputs seen with extracellular stimulation (*a–d*) and dual impalements (*e–h*). *a*, Schematic positions of neuron (same neuron as in Fig. 1) and stimulating electrode (radial in layer 5) for the input described in *b–d* and *i* (1,200 trials recorded). *b*, Averaged EPSP shows small amplitude with paired-pulse faciitation. Scale bar, 20 ms, 200 μV. *c*, Amplitude histograms of baseline noise (hatched bars) and responses to first (filled circles) and second pulses (open squares). The response to the second stimulus (at 15 ms delay) is facilitated relative to the first ($\sigma_n = 75\,\mu V$, $\mu_{s1} = 402\,\mu V$, $\sigma_{s1} = 187\,\mu V$, $\mu_{s2} = 687\,\mu V$, $\sigma_{s2} = 181\,\mu V$; CV of pulse 1 is 42.6%). *d*, Paired-pulse scattergram showing facilitation (more points above the diagonal than below); the response to each stimulus is highly variable. e, Schematic positions of presynaptic layer 6 neuron and postsynaptic spiny stellate neuron for the dual-recording synaptic connection described in *f–h* (1,300 trials recorded). Presynaptic neurons when recovered were all layer 6 pyramidal neurons; postsynaptic neurons were either spiny stellate neurons or layer 4 pyramidal neurons. *f*, Averaged EPSP shows small amplitude with paired -pulse facilitation. Scale bar, 20 ms, 200 μV. *g*, Amplitude histograms of baseline noise (hatched bars) and responses to first (filled circles) and second pulses (open squares). The second response (31 ms mean delay) is facilitated relative to the first ($\sigma_n = 133\,\mu V$, $\mu_{s1} = 308\,\mu V$, $\sigma_{s1} = 267\,\mu V$, $\mu_{s2} = 533\,\mu V$, $\sigma_{s2} = 262\,\mu V$; CV of pulse 1 is 75.2%). *h*, Paired-pulse scattergram showing facilitation and variability of response to each stimulus. *i*, Facilitation (100 × pulse 2/pulse 1) of the minimal stimulation input (open circles) described in *a–d* as a function of interpulse interval (200 trials per interval); facilitation is maximal (71%) at 15 ms delay. Dual-impalement data (filled squares) from the connection in *e–h* shows a similar dependence of facilitation on interpulse interval.

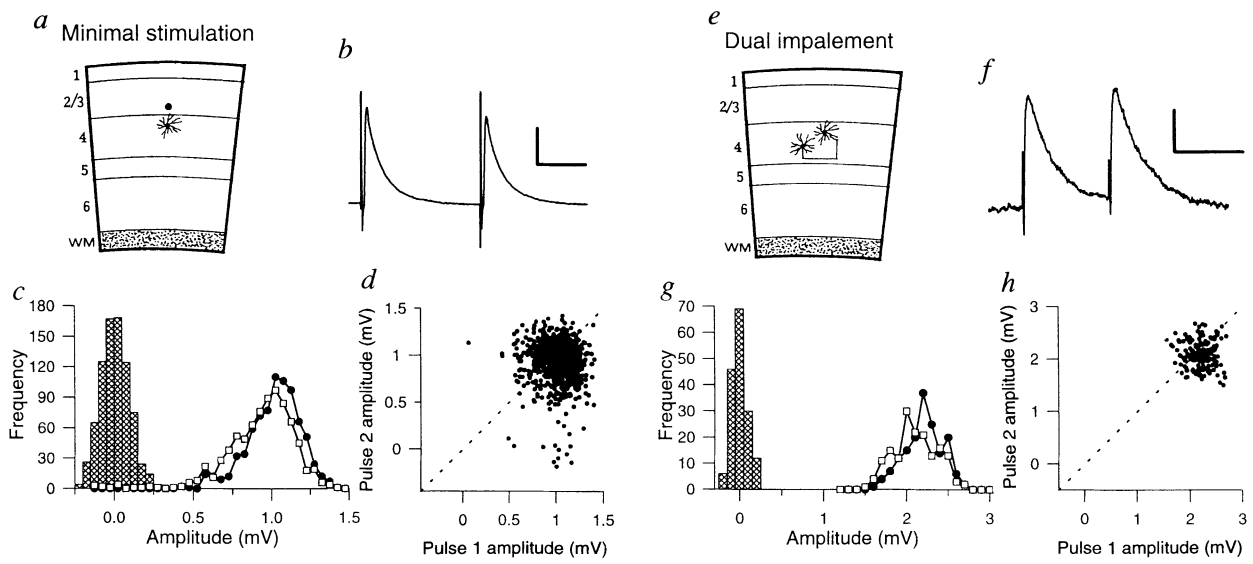

FIG. 3 Class 2 inputs. Characteristics of class 2 synaptic inputs seen with extracellular stimulation (*a–d*) and dual impalements (*e–h*). *a*, Schematic positions of neuron (same neuron as in Fig. 1) and stimulating electrode (radial in layer 3) for the input described in *b–d* (800 trials recorded). *b*, Averaged EPSP shows an intermediate amplitude response to both pulses. Scale bar, 20 ms, 400 μV. *c*, Amplitude histograms of baseline noise (hatched bars) and responses to first (filled circles) and second pulses (open squares). The response to the second stimulus (at 50 ms delay) is slightly decreased in amplitude and similar in variation to the first ($\sigma_n = 92\,\mu V$, $\mu_{s1} = 1{,}015\,\mu V$, $\sigma_{s1} = 169\,\mu V$, $\mu_{s2} = 932\,\mu V$, $\sigma_{s2} = 218\,\mu V$; CV of pulse 1 is 13.9%). *d*, Paired-pulse scattergram shows that stimulation rarely fails to evoke a response to both stimuli, and the second response is similar to the first; both responses show variation in amplitude. *e*, Schematic positions of presynaptic and postsynaptic neurons in layer 4 for the dual-recording synaptic connection described in *f–h* (600 trials recorded). Both neurons were morphologically confirmed spiny stellate neurons (somata 55 μm apart laterally). *f*, Averaged EPSP again shows similar amplitude responses to both pulses. Scale bar, 40 ms, 800 μV. *g*, Amplitude histograms of baseline noise (hatched bars) and responses to first (filled circles) and second pulses (open squares). The response to the second stimulus (at 54 ms mean delay) is slightly decreased in amplitude and similar in variation to the first ($\sigma_n = 88\,\mu V$, $\mu_{s1} = 2{,}205\,\mu V$, $\sigma_{s1} = 226\,\mu V$, $\mu_{s2} = 2{,}097\,\mu V$, $\sigma_{s2} = 259\,\mu V$; CV of pulse 1 is 9.4%). *h*, Paired-pulse scattergram shows the second response is essentially similar to the first.

integrals and cell input resistances[27], we calculated the number of channels opening during the response to produce each EPSP, assuming that the postsynaptic receptors of cat and rat visual cortical spiny neurons have similar channel conductances and mean open times, about 9 pS and 1.9 ms, respectively[28]. Class 1 EPSPs require 428 ± 302 channels ($n = 14$); class 2, 280 ± 171 ($n = 14$); and class 3, 79 ± 39 ($n = 8$). Thus class 1 responses probably involve multiple synaptic contacts, all with extremely high release probability, whereas class 2 and class 3 EPSPs are probably multiquantal with moderately high and low release probabilities, respectively. Inputs with some class 1 characteristics have recently been reported in rat visual cortex[20].

There is considerable support for the view that the basic structure of the simple receptive field is established by the pattern of thalamic innervation[1–6]. However, our data suggest that thalamic excitation by powerful class 1 EPSPs will be amplified by the more numerous synaptic connections from adjacent layer 4 neurons. Additionally, temporally sensitive, potentiating synapses from layer 6 pyramidal neurons, which provide the major excitatory pathway to layer 4, can augment and modulate thalamic signal transmission[23,24]. These recurrent cortical circuits may have several functions, including contrast gain control[10], extraction of signals from incomplete or noisy data[29], and context-dependent receptive-field modifications[11,12]. □

Received 1 April; accepted 21 May 1996.

1. Hubel, D. H. & Wiesel, T. N. *J. Physiol., Lond.* **160,** 106–154 (1962).
2. Chapman, B., Zahs, K. R. & Stryker, M. P. *J. Neurosci.* **11,** 1347–1358 (1991).
3. Reid, R. C. & Alonso, J.-M. *Nature* **378,** 281–284 (1995).
4. Ferster, D., Chung, S. & Wheat, H. *Nature* **380,** 249–252 (1996).
5. Hubel, D. H. *Nature* **380,** 197–198 (1996).
6. Das, A. *Neuron* **16,** 477–480 (1996).
7. Garey, L. J. & Powell, T. P. *Proc. R. Soc. Lond.* B **179,** 41–63 (1971).
8. Peters, A. & Payne, B. R. *Cereb. Cortex.* **3,** 69–78 (1993).
9. Ahmed, B., Anderson, J. A., Douglas, R. J., Martin, K. A. C. & Nelson, J. C. *J. comp. Neurol.* **341,** 39–49 (1994).
10. Sclar, G. & Freeman, R. D. *Expl. Brain Res.* **46,** 457–461 (1982).
11. Gilbert, C. D. & Wiesel, T. N. *Vision Res.* **30,** 1689–1701 (1990).
12. Sillito, A. M., Grieve, K. L., Jones, H. E., Cudeiro, J. & Davis, J. *Nature* **378,** 492–496 (1995).
13. LeVay, S. & Gilbert, C. D. *Brain Res.* **113,** 1–19 (1976).
14. Lund, J. S., Henry, G. H., Macqueen, C. L. & Harvey, A. R. *J. comp. Neurol.* **184,** 599–618 (1979).
15. Gilbert, C. D. & Wiesel, T. N. *Nature* **280,** 120–125 (1979).
16. Martin, K. A. C. & Whitteridge, D. *J. Physiol., Lond.* **353,** 463–504 (1984).
17. Anderson, J. A., Douglas, R. J., Martin, K. A. C. & Nelson, J. C. *J. comp. Neurol.* **341,** 25–38 (1994).
18. Hirsch, J. *J. Physiol., Lond.* **483,** 183–199 (1995).
19. Allen, C. & Stevens, C. F. *Proc. natn. Acad. Sci. U.S.A.* **91,** 10380–10383 (1994).
20. Volgushev, M., Voronin, L. L., Chistiakova, M., Artola, A. & Singer, W. *Eur. J. Neurosci.* **7,** 1751–1760 (1995).
21. Everitt, B. S. *Cluster Analysis* 3rd edn (Edward Arnold, London, 1993).
22. Andreason, M. & Hablitz, J. J. *J. Neurophysiol.* **72,** 326–336 (1994).
23. Ferster, D. & Lindstrom, S. *J. Physiol., Lond.* **367,** 233–252 (1985).
24. Grieve, K. L. & Sillito, A. M. *Expl. Brain Res.* **87,** 521–529 (1991).
25. Mason, A., Nicoll, A. & Stratford, K. *J. Neurosci.* **11,** 72–84 (1991).
26. Stevens, C. R. in *Large-scale Neuronal Theories of the Brain* (eds Koch, C. & Davis, J. L.) 239–255 (MIT Press, Cambridge, MA, 1994).
27. Jack, J. J. B., Noble, D. & Tsien, R. W. *Electrical Current Flow in Excitable Cells* (Clarendon, Oxfod, 1975).
28. Hestrin, H. *Neuron* **11,** 1083–1091 (1993).
29. Douglas, R. J., Koch, C., Mahowald, M., Martin, K. A. C. & Suarez, H. H. *Science* **269,** 981–984 (1995).

ACKNOWLEDGEMENTS. We thank A. Larkman for valuable adivce and for reading the manuscript; D. Fleming for animals; and B. Ahmed, J. Anderson, V. Meskenaite and C. Nelson for morphological advice and help. K.T.-H. is a Wellcome Trust prize student. This work was supported by The Wellcome Trust, The Royal Society and The Medical Research Council.

CORRESPONDENCE and requests for materials should be addressed to K.J.S. (e-mail: kenneth.stratford@physiol.ox.ac.uk).